Spectrum of Luminescence from Laser-Created Bubbles in Water

Ohan Baghdassarian, Han-Ching Chu, Bernd Tabbert, and Gary A. Williams

Department of Physics and Astronomy, University of California, Los Angeles, California 90095
(Received 4 February 2001)

The spectrum of the luminescence emitted at the collapse of single laser-induced bubbles in water is measured for different maximum bubble radii. Bubbles as large as 2 mm show a molecular OH* band at 310 nm in the spectrum, which otherwise can be fitted approximately with a blackbody curve at a temperature of 7800 K. This finding provides a connection between the light emission of single bubbles and multibubble sonoluminescence, since in the latter case the same molecular band is observed. Surface instabilities are observed in the larger bubbles, and may be connected with the OH* emission.

The energy focusing of a collapsing bubble in water can lead to the emission of photons of energy 6 eV and higher, the phenomenon observed in single-bubble sonoluminescence (SBSL) [1,2]. The exact mechanism of the luminescence from single bubbles trapped in a sound field is still debated [3,4], in part because of the challenges presented in probing the light-emitting region, which is thought to be less than a few micrometers in diameter. It is of interest to scale up the bubble size in order to compress more mass and study consequently larger hot spots. There is also the puzzle of understanding the relationship of SBSL to multibubble sonoluminescence (MBSL) [5,6], which is light emission from the cloud of bubbles in a fluid cavitated continuously with an intense sound field. The spectrum of MBSL [6] shows an emission band from the OH* molecular complex which starts at 306.4 nm and peaks near 310 nm, while SBSL shows only a smooth continuum spectrum that increases into the ultraviolet without any obvious lines [7,8].

We report measurements of the spectrum of the light emission from single collapsing laser-induced bubbles in water that have different maximum radii. Figure 1 shows the OH* spectral band emerging from a continuous spectrum with increasing bubble size, the same band previously found in the optical spectra of MBSL. In the remainder of the paper we compare the features of these spectra of laser-created bubbles with the spectra of MBSL and SBSL, and discuss the possibility that instabilities in the bubble shape play a role in the occurrence of spectral lines for large bubbles.

The bubbles are created from a focused laser pulse that initially vaporizes the water, giving rise to a bubble that first expands, reaches a maximum radius, and then collapses in a time of order $100-400$ μs that is directly proportional to the maximum radius [9,10]. The exact composition of the gas being compressed in the bubble collapse is not known, but probably consists primarily of atomic and molecular hydrogen and oxygen, and any water vapor that is unable to condense onto the bubble wall. The luminescence pulse is emitted precisely at the minimum-radius collapse point, and the width of the pulse is several nanoseconds, increasing as the maximum

bubble size increases [10]. The range of bubble radii that can be created by this method (0.2–2 mm) is much larger than the bubbles of SBSL, which have a maximum radius about 50 μm.

A Nd:YAG laser producing 6 ns pulses with a maximum energy of 600 mJ at 1064 nm is collimated and focused to a point about 10 μm in diameter to cavitate the high purity water sample, as previously described in Ref. [10]. The laser energy is adjusted to the threshold for creating just a single bubble, estimated to be of order 100 mJ. The water is inside a sealed cell having quartz windows for monitoring the emitted light with a photomultiplier, and the radius of the bubble versus time is monitored by a shadowgraph technique and by pulsed-laser photography through a long-distance microscope. To obtain a spectrum, light emitted from the bubble region is also collected and collimated by a MgF$_2$-coated paraboloidal mirror. A second paraboloid mirror focuses the collimated beam into the entrance slits of a 0.3 m spectrometer with a gateable
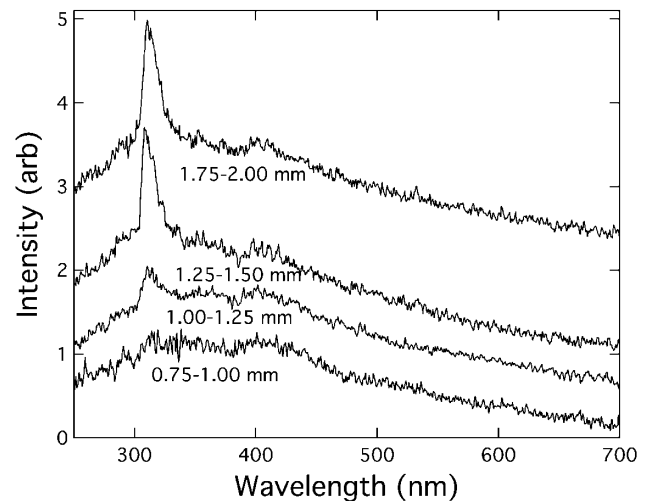
FIG. 1. Spectra of the collapse luminescence as the bubble size is increased, showing the growth of the OH* band at 310 nm. These are averaged over 40–50 bubbles, having maximum radii in the range indicated, and have been offset in the vertical direction to separate them (they are normalized to all coincide with the lowest curve between 500–700 nm).

intensified charge-coupled device (ICCD) detector. To reject light at higher order, long-pass filters at either 300 or 500 nm are placed in front of the spectrometer. The spectral response from 200–800 nm is calibrated for detection efficiency against a tungsten-halogen lamp and a deuterium lamp, with and without the cell in place to correct for the absorption of the water and windows. Two different gratings are used, having a spectral range on the ICCD detector of about 200 nm (2 nm resolution) and 30 nm (0.3 nm resolution), respectively. To get a sufficient signal for a spectrum it is necessary to average the light from 40–50 bubbles over a small range of bubble sizes.

We find that for small bubbles the spectrum of the collapse luminescence (the lowest curves in Figs. 1 and 2) has a smooth continuum which peaks at about 380 nm and then decreases into the ultraviolet. This is approximated by a blackbody spectrum with a temperature of 7800 K (solid curve in Fig. 2), consistent with compressional heating of the gas in the bubble and creation of a thermal plasma. However, as the bubble size is increased the OH* molecular band becomes readily apparent in the spectrum (Fig. 1), providing a link with the phenomenology of multibubble sonoluminescence, which also can have bubble sizes in the millimeter range [5,6]. To check the time dependence of the OH* band the luminescence is viewed with two photomultipliers, one with a filter which only passes light between 303 and 313 nm. There appears to be little difference between the two pulses, so to within an uncertainty of 1–2 ns it appears that the band is coincident with the continuum. We cannot resolve the spatial origin of the different parts of the spectrum; it is possible that the OH* band could come from the cooler region at the bubble

surface, and the continuum from the hotter center of the bubble. We find little detectable change in the continuum spectrum with bubble size even for the largest bubbles.

The ionization of the water by the YAG pulse creates an initial plasma 50–80 μm in radius that emits a bright pulse of light. The pulse has a duration of about 100 ns, with then a weak tail decaying over several μs. The spectrum of this pulse, plotted in Fig. 2, shows an intensity rising smoothly into the ultraviolet with no visible atomic lines. This compares well with a blackbody spectrum at a temperature of 16 000 K (the dashed curve in Fig. 2). Similar blackbody spectra have been observed previously for laser-induced plasmas in water [11], where a blackbody temperature of 10 000 K was found for a smaller incident laser power of 5 mJ. By gating the ICCD just after the main pulse, in the tail region, we find that the spectrum then consists primarily of the feature from the OH* band at 310 nm. The OH* is presumably formed as a product of the plasma recombination process.

Since SBSL also shows a spectrum rising smoothly into the ultraviolet [7], we decided to compare an SBSL spectrum directly with our results on the initial plasma. An acoustical SBSL cell at 33 kHz was mounted into the sample region of our setup, filled with water at 150 torr partial pressure of dissolved air. This cell was carefully aligned to center the acoustically trapped bubble to the same point where the laser created the plasma in the previous experiment. Figure 1 shows the spectrum resulting from integrating several seconds of the SBSL pulses. This appears to have nearly the same wavelength dependence as that of the initial plasma, i.e., that of a blackbody at 16 000 K. SBSL spectra were initially interpreted in terms of blackbody emission, but doubts arose that such a small hot spot could be completely opaque to photons [3,12]. Our result, and a reanalysis of other SBSL spectra [13], supports a conclusion that SBSL is at least approximated by blackbody emission from a weakly ionized thermal plasma.

Our previous results on laser-induced bubbles showed that the intensity of the luminescence was independent of the presence or absence of dissolved gases in the water [10]. We have verified that this also holds for the emission spectra of Figs. 1 and 2; no difference at all could be seen between water samples completely degassed and those left with the ambient 1 bar dissolved air. The results shown in this paper are all for the ambient 1 bar samples.

We find that adding 0.1 molar NaCl to the water leads to the appearance of sodium D lines at 589 nm, in both the initial plasma emission (as also seen in Ref. [11]) and the collapse luminescence of bubbles of all sizes. In the initial plasma pulse the two D lines are broadened so much they are not resolved, while 1 μs later in the colder tail they become distinct. They are also not resolved in the collapse emission. The appearance of the D lines provides a further connection to MBSL, where they are also observed [6] with the addition of salt, but have never been seen in
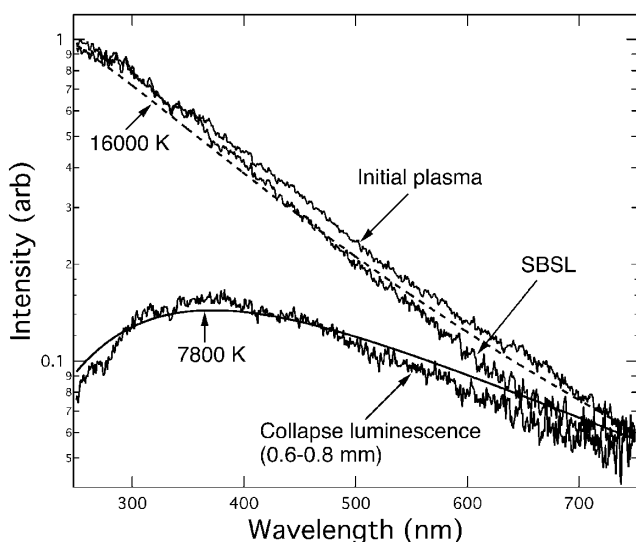
FIG. 2. Spectral intensity versus wavelength for the luminescence from small bubbles (0.6–0.8 mm maximum radius), from the initial laser-induced plasma, and from an SBSL cell positioned at the point where the laser bubbles are created. Intensities have been scaled arbitrarily between the different curves.

SBSL. In our case of laser-induced bubbles the appearance of the lines is perhaps not surprising, since an appreciable quantity of salt is ionized in the initial laser plasma, and then remains in the bubble for the subsequent compressional heating, plasma formation, and emission at the collapse point. There is no obvious mechanism for getting salt into the interior of an SBSL bubble since the vapor pressure of the NaCl is so small.

The bubble and the collapse luminescence can be imaged by viewing the microscope output with the ICCD camera. By backlighting the bubble with a train of 200 ns pulses from an argon-ion laser, multiple images of the bubble can be captured on a single frame, along with the luminescence flash, as shown in Fig. 3. For smaller bubbles the collapse is spherical and centered on the lu-
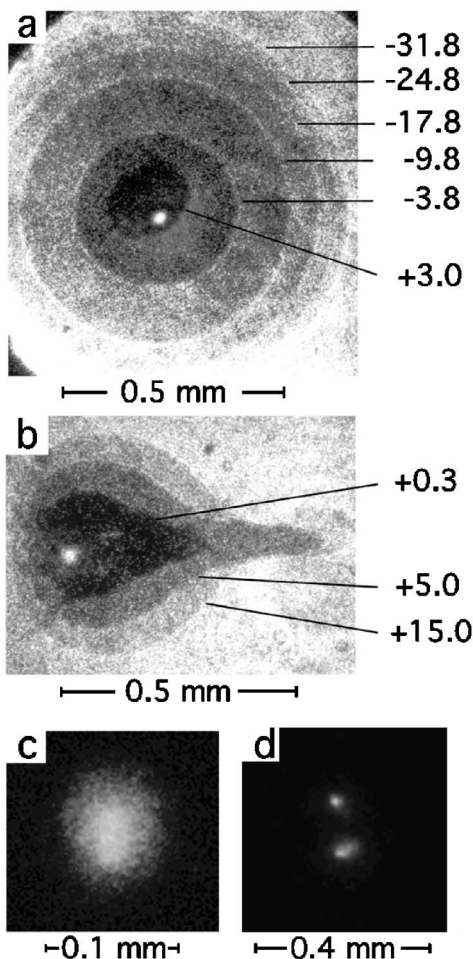
FIG. 3. Photographs of the bubbles, backlit with 200 ns pulses from an Ar-ion laser. (a) The luminescence from the hot spot is visible in the center of a collapsing bubble of maximum radius 0.45 mm, shown for five exposures on the collapse (negative times in μs from the luminescence pulse at 92 μs) and one on the asymmetric rebound (positive time). (b) Three exposures of a bubble after the collapse point, showing the formation of a jet-like structure on the rebound. (c) Enlarged view of the luminescence hot spot from a bubble with 0.8 mm maximum radius. (d) Double flash from a split bubble of maximum radius 1 mm.

minescence pulse, as seen in Fig. 3a, but the rebounding bubble just past the collapse is always quite asymmetric initially, as seen in Fig. 3a at $+3.1$ μs past the collapse point. It only regains a nearly spherical shape tens of μs later. This behavior is probably the result of the high acceleration of the bubble wall at the collapse point, giving rise to Rayleigh-Taylor instabilities [14]. Occasionally we observe that these instabilities are strong enough that jet-like structures are formed in the rebound region, as shown in Fig. 3b. Figure 3c shows an enlarged view of the emission hot spot, which appears to be fairly uniform with a diameter of about 25 μm (full width at half maximum intensity), in agreement with previous measurements [15].

For bubbles whose maximum radius is greater than about 1 mm a further instability becomes apparent: just before the collapse point they are often seen to split in two (similar to the pressurized smaller bubbles of Ref. [10]), with each one giving off a luminescence pulse, as shown in Fig. 3d. The time between the two pulses varies with each split-bubble event, but is generally of order 10–20 ns. The spectra of these split bubbles is identical to those of Fig. 1 (where only single-pulse events were selected), showing again the OH* band.

It seems quite possible that the onset of the OH* emission for bubbles larger than 1 mm could be connected with the strong surface instabilities we observe for these bubbles. Similar arguments were advanced in Ref. [6] for the case of MBSL, and it has also been proposed [16] that jets across the bubble interior could greatly affect the plasma formation. It is clear that further observations closer to the collapse point using faster laser pulses will be needed to check this in detail.

The radius of the bubble versus time can be monitored with a shadow technique [10]. To get higher resolution in the region of the collapse minimum, we have partially focused the backlighting laser beam to a spot size of about 0.6 mm. Figure 4a shows data for a bubble whose maximum radius is 1.2 mm. The beam is disrupted by the outgoing acoustic shock wave very close to the collapse point, but enough of the dynamics can be obtained before and after this that fits can be made to the Rayleigh-Plesset equations [17] for the bubble dynamics, shown as the solid line. From the fit parameters of $R_{min} = 0.035$ mm and a bubble pressure of 0.5 mbar at R_{max}, the temperature of the compressed gas can be obtained (assuming crudely that the specific-heat ratio $\gamma = 7/5$), as shown in Fig. 4b. The thermal ionization of the gas is also shown, as calculated from the Saha equation [18], making the assumption that the ionization potential is the 13.6 eV of atomic hydrogen. Since the ionization depends exponentially on the temperature it is appreciable for only a short time; the half-width of the weak ionization in Fig. 4b is 40 ns, which compares to our measured pulse widths of about 8 ns for a bubble this size. The light emission would occur only when the plasma is present, since only then does the opacity become appreciable [3,12]. The calculated maximum
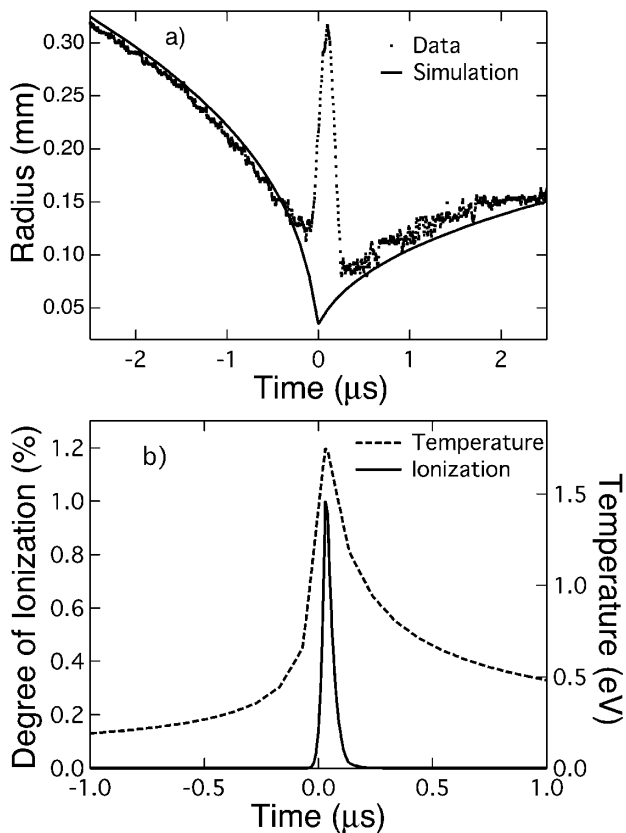
FIG. 4. (a) Bubble radius versus time near the collapse point, fit to Rayleigh-Plesset equations of motion (solid line). (b) Gas temperature in the bubble and ionization percentage, calculated from the fit parameters.

temperature of about 25 000 K is likewise larger than the blackbody temperature of 7800 K found above. This is a very crude calculation that can only be expected to yield order-of-magnitude estimates; we hope this data will stimulate more detailed and accurate theories of these freely collapsing bubbles.

In summary, we have measured the spectrum of luminescence from collapsing laser-created bubbles in water. A continuum is found that approximates a blackbody spectrum at 7800 K; however, as the bubble size is increased a molecular band from OH* becomes apparent in the spectrum. This provides a connection to multibubble sonoluminescence [6] and to unstable SBSL [8], where the same line is observed. The appearance of the OH* band may be related to the unstable dynamics of these larger bubbles in the vicinity of the collapse point. Further work will be needed to understand the details of the plasma creation process, and how the the bubble-wall instabilities might affect it.

[1] D. Gaitan, L. Crum, R. Roy, and C. Church, J. Acoust. Soc. Am. **91**, 3166 (1992).

[2] B. Barber, R. Hiller, R. Löfstedt, S. Putterman, and K. Weninger, Phys. Rep. **281**, 65 (1997).

[3] S. Hilgenfeldt, S. Grossman, and D. Lohse, Nature (London) **398**, 402 (1999); Phys. Fluids **11**, 1318 (1999).

[4] S. Putterman, P. Evans, G. Vasquez, and K. Weninger, Nature (London) **409**, 782 (2001); S. Hilgenfeldt, S. Grossman, and D. Lohse, *ibid.*, 783 (2001).

[5] A. Walton and G. Reynolds, Adv. Phys. **33**, 595 (1984).

[6] T. Matula, R. Ronald, P. Mourad, W. McNamara, and K. Suslick, Phys. Rev. Lett. **75**, 2602 (1995).

[7] R. Hiller and S. Putterman, Phys. Rev. Lett. **75**, 3549 (1995); R. Hiller, Ph.D. thesis, UCLA, 1997 (unpublished).

[8] Recently discrete lines have been found in SBSL when it is run in regimes where the bubble motion can become unstable: Y. Didenko, W. McNamara, and K. Suslick, Nature (London) **407**, 877 (2000); J. Young, J. Nelson, and W. Kang, Phys. Rev. Lett. **86**, 2673 (2001). Direct observation of instabilities in bubbles driven just below the lower threshold to get SBSL is reported in Y. Tian, J. Ketterling, and R. Apfel, J. Acoust Soc. Am. **100**, 3976 (1996).

[9] A. Buzukov and V. Teslenko, Sov. Phys. JETP Lett. **14**, 189 (1971).

[10] O. Baghdassarian, B. Tabbert, and G. A. Williams, Phys. Rev. Lett. **83**, 2437 (1999).

[11] D. Stolarski, J. Hardmann, C. Bramlette, G. Noojin, R. Thomas, B. Rockwell, and W. Roach, *Proceedings of Laser Tissue Interaction VI,* SPIE Proceedings Vol. 2391 (SPIE-International Society for Optical Engineering, Bellingham, WA, 1995), p. 100.

[12] W. Moss, D. Clarke, and D. Young, Science **276**, 1398 (1997).

[13] G. Vasquez, C. Camara, S. Putterman, and K. Weninger (to be published).

[14] Instabilities and jets have been observed in the rebound regime for freely collapsing cm-sized bubbles in T. B. Benjamin and A. T. Ellis, Philos. Trans. R. Soc. London A **260**, 221 (1966).

[15] C. Ohl, T. Kurz, R. Geisler, O. Lindau, and W. Lauterborn, Philos. Trans. R. Soc. London A **357**, 269 (1999).

[16] A. Prosperetti, J. Acoust. Soc. Am. **101**, 2003 (1996).

[17] R. Lofstedt, B. Barber, and S. Putterman, Phys. Fluids A **5**, 2911 (1993).

[18] E. Fermi, *Thermodynamics* (Dover, New York, 1936).